JOURNAL OF CATALYSIS 145, 16–26 (1994)

# Site Suppression and Pore Choking in the Deactivation of Nickel–Molybdenum Coal-Liquid Hydrotreatment Catalyst

Dady B. Dadyburjor and Ajoy P. Raje

*Department of Chemical Engineering, West Virginia University, Morgantown, West Virginia 26506-6101*

Received March 15, 1993; revised July 21, 1993

**Coal-liquid hydrotreatment (HT) catalysts deactivate by active site suppression and/or pore choking. The relative importance of these two mechanisms is quantitatively assessed by evaluation of the intrinsic reaction rate constant, $k_{int}$, and $D_{eff}$, the effective diffusivity, for catalysts removed at various age levels from a commercial HT unit. The two parameters are obtained from the observed rate constants for the hydrodesulfurization of thiophene as a function of temperature (between 180 and 550°C) using a modified version of the Constant–Deactivation Arrhenius Plot technique. At catalyst ages less than 200 lb. resid/lb. catalyst, pore choking is the dominant mechanism of deactivation. At higher catalyst ages, while both pore choking and active site suppression are responsible for catalyst deactivation, the contribution of pore choking is greater than the contribution of site suppression. These results do not change qualitatively with temperature.** © 1994 Academic Press, Inc.

## INTRODUCTION

Declining crude oil reserves and an overdependence on foreign oil supplies have led to coal liquefaction being considered as an alternative to producing synthetic liquid fuels. Since the late 1970s, coal liquefaction processes have developed into integrated two-stage processes (1), with coal being hydroliquefied in the first stage and the coal liquids obtained being hydrotreated in the second stage. The principal reactions involved in hydrotreatment (HT) are hydrodesulfurization (HDS), hydrodenitrogenation (HDN), and hydrodeoxygenation (HDO). HT converts the sulfur-, nitrogen-, and oxygen-containing heteroatom compounds present in coal liquids to hydrocarbons and hydrogen sulfide, ammonia, and water respectively.

Catalysts commonly used for HT are a mixture of nickel and molybdenum oxides supported on alumina. The catalyst is sulfided in-situ to the active state. During HT, these catalysts deactivate rapidly and must be replaced in 1 to 6 months. The deactivation is due to the deposition of coke and metals on the catalyst. Coke is formed by the cracking of hydrocarbons present in coal liquids. Metals originate either from the mineral matter present in coal or from organometallic constituents. Other deactivation mechanisms, for instance, sintering or changes in active phase of the catalyst, are not significant under typical HT reaction conditions (2). The heteratom compounds involved in the principal reactions of the HT process do not by themselves deactivate the catalyst (2). Coke deposits are distributed uniformly inside the catalyst pellet while metals deposit preferentially around the periphery of the catalyst pellet (2). Iron and titanium are the major constituents of the metal deposits (3).

The coke and metal deposits lead to the suppression of active sites on the catalyst and/or choking of the catalyst pores. Active site suppression causes the intrinsic rate constant per unit weight of the catalyst, $k_{int}$, to decrease. Pore choking causes a decrease in $D_{eff}$, the effective diffusivity of the reactants and products in the catalyst pellet. Both of these deactivation mechanisms lead to a decrease in the overall observed reaction rate constant, $k_{obsd}$.

The objective of the present study is to determine the relative importance of these two mechanisms—site suppression and pore choking—in the deactivation of HT catalysts. Knowledge of the deactivation mechanism can suggest ways to modify the catalyst to increase its active life.

The relative importance of the two mechanisms can be determined by evaluating both $k_{int}$ and $D_{eff}$ of the catalyst as deactivation proceeds. However, these two quantities are strongly coupled in the observed rate constant, $k_{obsd}$, and cannot be easily separated. For reaction and diffusion inside a porous catalyst pellet, $k_{obsd}$ is given by (4)

$$k_{obsd} = \eta\, k_{int}, \qquad [1]$$

where the effectiveness factor, $\eta$, accounts for pore diffusion and is, in general, a complicated function of the Thiele modulus, $\phi$ (4). The Thiele modulus in turn depends on $k_{int}$, $D_{eff}$ and the geometry and dimensions of the pellet.

Some investigations have been carried out to measure $k_{int}$ and $D_{eff}$ for various spent catalyst samples from coal-liquid HT reactors. Guin *et al.* (5) measured $D_{eff}$ of spent



0021-9517/94 $5.00

catalysts by using inert compounds at room temperature. The results indicate a trend of decreasing diffusivity with age of the spent catalyst samples. Stephens and Stohl (6) measured the $k_{int}$ of spent catalyst samples by crushing the catalyst pellets and using them for pyrene hydrogenation at 300°C. Further, the observed rate constant was also measured for the whole (i.e., uncrushed) catalyst pellets. From the effectiveness factor so determined and the calculated Thiele modulus, the $D_{eff}$ of each catalyst sample was calculated. The results indicate that the value of $k_{int}$ of the catalyst samples decreases with catalyst age, whereas the value of $D_{eff}$ remains practically constant during HT. The trends in $D_{eff}$ with respect to catalyst age observed by the two investigations lead to contradictory conclusions about the role of pore choking in catalyst deactivation.

The technique used in this study—a modified version of the Constant-Coke Arrhenius Plot (CCAP) method (7)—determines the $k_{int}$ and $D_{eff}$ under actual reaction conditions, without using inert compounds and without altering the catalyst structure.

## THEORETICAL

### *Constant-Deactivation Arrhenius Plots (CDAP)*

The CCAP method (7) was originally proposed for evaluating the relative importance of site suppression and pore choking during coking of a catalyst. During HT, both coke and metal poisons deposit in the catalyst, hence the change in nomenclature from CCAP to CDAP. In the CCAP procedure, the fresh catalyst is subjected to the reaction under study over a sufficiently wide range of temperatures. At each temperature, the value of the observed rate constant is obtained at increasing coke contents of the catalyst as it deactivates. The observed rate constants are then recast into a series of Arrhenius plots, each at a constant coke level on the catalyst pellet. Such a procedure has been used (8) to evaluate cumene cracking over a zeolite-Y catalyst. The results indicate that both temperature and coke level affect the relative importance of site suppression and pore choking.

This procedure is modified in the present study. Since the HT of coal liquids cannot easily be carried out in a bench-scale apparatus to simulate conditions in an actual industrial-scale HT reactor, spent catalyst samples have been used. These samples have been deactivated to different extents in an industrial HT reactor, and have differing amounts of coke and metal deposits.

We have carried out the HDS of a sulfur-containing compound, thiophene, over each of these catalyst samples. The predeactivated catalyst samples do not deactivate further during thiophene HDS, since heteroatom compounds do not deactivate the catalyst, as mentioned above. Hence, steady-state observed rate constants can be readily obtained at various temperatures over a particular predeactivated catalyst sample. This yields an Arrhenius plot at a constant level of deactivation (coke and metal deposits). The procedure can be repeated over catalyst samples predeactivated to different extents to obtain Arrhenius plots at several (constant) deactivation levels of the catalyst.

If the Arrhenius plots (at a constant deactivation level) are obtained over a sufficiently wide temperature range, asymptotes can be drawn at low and at high temperatures (9). At sufficiently low temperatures, pore diffusion limitations are negligibly small, and the intrinsic kinetics control the overall rate of reaction. In this region, the effectiveness factor, $\eta$, is independent of the Thiele modulus and has a value of unity. Therefore, at low temperatures,

$$k_{obsd} = k_{int}. \quad [2]$$

The slope of the low-temperature asymptote, $m_L$, gives the activation energy of reaction, $E_k$,

$$E_k = m_L R, \quad [3]$$

where $R$ is the gas constant.

At high temperatures, pore diffusion exerts a strong influence on the overall reaction rate, giving a second limiting region in the Arrhenius plot, through which a high-temperature asymptote can be drawn. The functional dependence of the effectiveness factor on the Thiele modulus in this region depends on the intrinsic kinetics of the reaction under study and is described below.

### *First-Order Kinetics*

For the simplest case of a first-order, irreversible reaction (9), the effectiveness factor at sufficiently high temperatures is given by

$$\eta \approx 1/\phi \quad [4]$$

and the Thiele modulus is

$$\phi = L(\rho_p k_{int}/D_{eff})^{1/2}, \quad [5]$$

where $\rho_p$ is the density of the catalyst pellet and $L$ is a length parameter dependent on the dimensions and shape of the catalyst pellet. Therefore, the observed rate constant is given by

$$k_{obsd} = (1/L)(k_{int}D_{eff}/\rho_p)^{1/2}. \quad [6]$$

The slope of the high-temperature asymptote, $m_H$, is then related to the average of the activation energies for reac-

tion, $E_k$, and for diffusion, $E_D$, and to the gas constant, $R$, as

$$m_H = (E_k + E_D)/(2R). \quad [7]$$

The activation energy for diffusion, $E_D$, is small (1–4 kcal/mole) as compared to $E_k$ (20–40 kcal/mole). Therefore, the slope of the high-temperature asymptote is approximately half the slope of the low-temperature asymptote

$$m_H \approx m_L/2. \quad [8]$$

From the low- and high-temperature asymptotes to the Arrhenius plot, the values of $k_{int}$ and $D_{eff}$ for the catalyst at a particular constant deactivation level, $\pi$, are given by

$$k_{int}(T, \pi) = A_L(T, \pi) \quad [9a]$$

$$D_{eff}(T, \pi) = L^2\rho_p A_H(T, \pi)^{1/2}/A_L(T, \pi). \quad [9b]$$

$A_L$ and $A_H$ are the values of the low- and high-temperature asymptotes, respectively, at the temperature, $T$, for the Arrhenius plot at a constant deactivation level, $\pi$. Similarly, $k_{int}$ and $D_{eff}$ can be evaluated at other deactivation levels from the Arrhenius plots at these levels.

To compare rate constants at different catalyst ages, the rate constants must all refer to the same weight of the catalyst pellet. However, the weight of the catalyst pellet increases during deactivation, due to the coke and metal deposits. Therefore, the value of the rate constant needs to be adjusted to refer to some constant (invariant) weight of the catalyst pellet. The equivalent weight of the fresh catalyst is chosen as the reference weight. The observed rate constant for the deactivated catalyst per unit weight of fresh catalyst, $k_{obsd}$, is then given in terms of the value per unit weight of the deactivated catalyst, $k'$ as

$$k_{obsd} = k'/(1 - \text{wt fraction coke} - \text{wt fraction metal compound}). \quad [10]$$

The deactivation level of the least-deactivated catalyst analyzed is assigned to be the reference deactivation level, $\pi_{ref}$. Then the ratios of $k_{int}$ at a particular deactivation level to $k_{int}$ at $\pi_{ref}$ gives a quantitative measure of the amount of site suppression between the two deactivation levels. Denoting this ratio by $R_k$, we get

$$R_k(T) = k_{int}(T, \pi)/k_{int}(T, \pi_{ref}). \quad [11]$$

Similarly, the ratio of $D_{eff}$ at a particular deactivation level to the $D_{eff}$ at $\pi_{ref}$, $R_D$, gives a quantitative measure of the amount of pore choking:

$$R_D(T) = D_{eff}(T, \pi)/D_{eff}(T, \pi_{ref}). \quad [12]$$

If $R_k$ and $R_D$ are compared at several catalyst ages, the relative importance of site suppression and pore choking during catalyst deactivation can be determined.

*Modifications to First-Order Analysis*

The HDS of thiophene, however, is not a simple first-order reaction. The HDS of thiophene yields the products butene and hydrogen sulfide according to the reaction

$$\text{thiophene} + 3H_2 \rightarrow \text{butene} + H_2S. \quad [13]$$

Satterfield and Roberts (10), Ihm *et al.* (11), and others have studied the kinetics of thiophene HDS and have proposed a second-order Langmuir–Hinshelwood rate expression

$$-r_T = k_{LH}P_TP_H/(1 + k_TP_T + k_SP_S)^2. \quad [14]$$

For this rate expression, the functional dependence of the effectiveness factor on the Thiele modulus is complicated (12). Hence, numerical analysis and curve-fitting techniques would be needed to determine $k_{int}$ and $D_{eff}$ from CDAP.

However, by a judicious choice of the experimental conditions, the simple algebraic analysis for first-order kinetics described above can still be used to obtain $k_{int}$ and $D_{eff}$. If a low concentration of thiophene (and hence product hydrogen sulfide) is maintained in the reactor, then the adsorption terms in the denominator of Eq. [14] can be neglected. In addition, if the mole fraction of thiophene is maintained much lower than the mole fraction of hydrogen in the reaction mixture, then the hydrogen partial pressure can be assumed constant. Thus, a pseudo-first-order assumption can be justified. This assumption has been verified over a wide range of thiphene conversions, and at several temperatures (13).

Further, in order to compare pseudo-first-order rate constants, the total pressure, $P_t$, and the hydrogen concentration, $C_H$, must be the same. This is not experimentally convenient, however, for the wide range of temperatures and catalyst deactivation levels over which the pseudo-first-order rate constants need to be measured. The rate constants, then, need to be adjusted so that they all refer to the same $C_H$ and the same $P_t$. In addition, the variation of $P_t$ affects $C_H$, and $P_t$ may also affect the value of $D_{eff}$.

Several adjustments must be made to the observed (pseudo-first-order) rate constant values so that they all refer to the same values of $C_H$ and $P_t$. For the case of hydrogen concentration, if the intrinsic kinetics control the rate of reaction, then the observed rate constant is

TABLE 1

**Properties of Fresh Shell 324M Catalyst (3)**

| | |
|---|---|
| Bulk density | 0.78 g/cm$^3$ |
| Pellet density | 1.38 g/cm$^3$ |
| Pore volume | 0.43 cm$^3$/g |
| Surface area | 180 m$^2$/g |
| Average pore dia | 115 Å |
| NiO | 3.4 wt% |
| MoO | 19.3 wt% |
| $Al_2O_3$ | 62.5 wt% |
| $Na_2O$ | 0.1 wt% |
| $SiO_2$ | <0.3 wt% |
| $P_2O_3$ | 5.7 wt% |

proportional to $C_H$, whereas the proportionality is to $C_H^{1/2}$ if diffusion exerts a strong influence on the reaction rate. For the case of total pressure, in the regime of strong diffusion influence, the dependence of the diffusion coefficient on $P_t$ varies with the diffusion mechanism—if Knudsen, then $D_{eff}$ is independent of $P_t$; if bulk, then $D_{eff}$ is inversely proportional to $P_t$. The three possibilities for the adjusted observed rate constant are given below for kinetic control, strong bulk-type-diffusion resistance, and strong Knudsen-type-diffusion resistance:

$$k_{kin} = k_{obsd}(C_{H,ref}/C_H) \quad [15]$$

$$k_{bulk} = k_{obsd}(C_{H,ref}/C_H)^{1/2}(P_t/P_{t,ref})^{1/2} \quad [16a]$$

$$k_{knud} = k_{obsd}(C_{H,ref}/C_H)^{1/2}. \quad [16b]$$

## EXPERIMENTAL PROCEDURE

### *Catalysts Used*

The predeactivated catalyst samples were obtained from the Advanced Coal Liquefaction Test Facility at Wilsonville, Alabama. The catalyst had previously been used in a HT reactor operating as the second stage in an integrated two-stage liquefaction process during Run #242 (14). The HT catalyst used in this process was Shell 324M, NiMo on alumina, having a unimodal pore structure. The catalyst is in the form of cylindrical extrudates, 1/32 in. in diameter and having an average length of 4 mm. Some properties of the fresh, i.e., unused, catalyst are given in Table 1 (3). The predeactivated samples were removed from the HT reactor at different times on stream. The deactivation, or age, of the catalyst samples is characterized as the pounds of residuum (resid or RSD) processed per pound of total catalyst in the reactor. Samples aged to different extents contain differing amounts of coke and metal deposits. Table 2 gives the ages, coke, and metal contents of the predeactivated catalyst samples used in this study (3).

During Run #242, Illinois #6 coal was used as the feed and the resulting coal liquids were processed in a critical solvent deasher before being fed to the HT reactor. Prior to use, the catalysts were presulfided *in situ* with 1% dimethyl disulfide in a coal-derived distillate. HT was carried out in an ebullated-bed reactor at an average temperature of 350°C and a hydrogen pressure of 2700–2800 psi. The temperature was increased periodically during the run to compensate for the declining activity of the catalyst. Fresh catalyst was added to the reactor, in amounts of 15 and 8 lbs. at catalyst ages of 244 and 253 lb. RSD/lb. cat, respectively. A much larger amount, 105 lbs. of catalyst, was added at a catalyst age of 584 lb. RSD/lb. cat. The initial weight of catalyst in the reactor was 411 lbs. Further details of Run #242 are given in Ref. (14).

Presulfiding of the catalyst with a coal-derived solvent resulted in coke deposition, and therefore deactivation of the catalyst, even before the start of the HT reaction (3). The least-deactivated (most active) catalyst sample analyzed in this study, WIL #1, was removed just after the sulfiding procedure was completed. The results of this study are, therefore, applicable to catalyst deactivation due to the HT reaction alone and do not depend upon the particular sulfiding procedure used in Run #242. Hence, deactivation due only to the HT reaction is analyzed here.

Further, samples with ages greater than 253 lb. RSD/lb. cat used in this work have been selected such that sufficiently large amounts of resid have been processed in the reactor after the relatively small addition (23 lb.) of fresh catalyst at that age. Finally, only those catalyst samples are analyzed that were removed before the addition of the large amount of fresh catalyst at 584 lb. RSD/lb. cat.

TABLE 2

**Age, Coke Content, and Metal Content of Predeactivated Shell 324M Catalyst (3)**

| Catalyst sample | Age (lb. RSD/lb. cat) | Coke[a] (wt%) | Fe | Ti (wt%) | Ca[b] |
|---|---|---|---|---|---|
| WIL #1 | 1 | 8.8 | 0.20 | 0.04 | 0.05 |
| WIL #2 | 54 | 9.8 | 0.20 | 0.20 | 0.10 |
| WIL #4 | 142 | 10.4 | 0.40 | 0.41 | 0.00 |
| WIL #5 | 192 | 10.0 | 0.51 | 0.62 | 0.17 |
| WIL #6 | 242 | 10.4 | 0.70 | 0.70 | 0.20 |
| WIL #9 | 368 | 9.8 | 0.60 | 0.60 | 0.20 |
| WIL #12 | 506 | 10.7 | 1.11 | 0.80 | 0.19 |

[a] Coke wt% is the sum of wt% of carbon, hydrogen, and nitrogen.
[b] Calcium wt% is estimated by the difference of wt% of total metals minus wt% of iron and titanium.

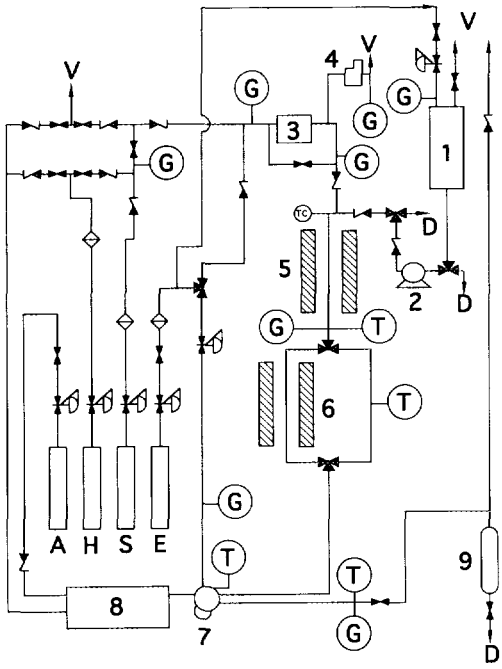


FIG. 1. Continuous-flow packed-bed reactor unit: (1) feed solution reservoir, (2) metering pump, (3) flowmeter, (4) relief valve, (5) preheater, (6) reactor, (7) sampling valve, (8) gas chromatograph, and (9) condenser; (A) air cylinder, (D) to drain, (H) hydrogen cylinder, (G) pressure gauge, (H) hydrogen cylinder, (S) 10% $H_2S$ in $H_2$ cylinder, (T) thermocouple, and (V) to vent.

*Experimental Apparatus*

A continuous-flow packed-bed reactor unit was used to characterize the activity of the predeactivated catalyst samples for thiophene HDS. A flowsheet of this unit is shown in Fig. 1. The reactor is a 3/8-in.-O.D. stainless-steel tube heated by an electric furnace. The temperature in the reactor is monitored by three thermocouples, one each at the inlet, outlet, and middle of the packed catalyst bed. The pressure is also measured at the inlet and outlet of the bed. A solution of 5 wt% thiophene in *m*-xylene (inert solvent) is fed by means of a metering pump, mixed with a controlled flow stream of hydrogen, and then passed through the preheater to vaporize the liquid completely. After reaction, the product stream passes through a heated six-port sampling valve (from Valco Instruments Co., Inc.). The vapor in the heated sampling valve is analyzed by a gas chromatograph (Shimadzu GC-Mini 2). The gas chromatograph has a flame ionization detector, and the column used for analysis of thiophene and products butene and butane is a "Super Q" column from Alltech Associates, Inc.

*Procedure*

Approximately 14 g of the catalyst was placed in the reactor for all pre-deactivated catalyst samples, except for sample WIL #1. For this (most active) sample, 8 g of the catalyst was diluted with 0.5-mm glass beads to make up an equivalent length of the reactor. The catalyst was pretreated by passing helium through the bed at 300°C and 15 psig pressure, at a flowrate of 400 ml/hr for 4 hr. A gas mixture of 10% $H_2S$ in $H_2$ was then used to sulfide the catalyst at 300°C and 15 psig pressure at a flowrate of 380 ml/hr for 4 hr.

The HDS of thiophene was carried out starting at the lowest temperature possible (consistent with an experimentally measurable formation of product butene) and subsequently at increasing temperatures. At each temperature, conversions were measured at two different flowrates of reactant thiophene, with at least three data points obtained at each flowrate. The same catalyst charge was used for activity measurements at all temperatures. Table 3 gives the reaction conditions employed in this study.

Since activity measurements were carried out at a wide range of temperatures (180–540°C), different sets of thiophene flowrates were used at different temperatures. The flowrate of hydrogen was varied proportionately, to maintain approximately 1 mole percent thiophene and 83 mole% hydrogen in the reactant mixture. This ensured that pseudo-first-order rate constants could be obtained from all runs.

At high temperatures and at high flowrates of thiophene, there was an appreciable pressure drop through the packed-bed reactor. This is taken into account in the analysis of the experimental data.

Experiments were also performed to test the validity of the first-order kinetic assumptions implicit in the CDAP analysis. Thiophene conversions were determined at four or five different flow rates and at several temperatures, covering a wide range of conversions. Experiments were also conducted using crushed catalyst samples, to confirm that the low-temperature rate constants obtained were actually in the kinetics-controlling regime.

## DATA ANALYSIS

At all temperatures, and for all the predeactivated catalyst samples analyzed, the products observed for the HDS of thiophene were butene and a small amount of butane. Conversions were calculated as the ratio of butene and

TABLE 3

**Reaction Conditions**

| | |
|---|---|
| Pressure at inlet of reactor | 3.5–11.5 atm |
| Temperature of reactor | 180–525°C |
| Flowrate of reactor feed | 5–200 ml/hr |
| Mole fraction of thiophene in reactor feed | 0.01 |
| Mole fraction of hydrogen in reactor feed | 0.80 |

butane formed to total moles of thiophene, butene, and butane in the product stream. Detailed total carbon balances were obtained for one catalyst, sample WIL #12, and were found to be greater than 93%, indicating that the calculated conversions are the same as conversions based on the disappearance of thiophene.

Since there was an appreciable pressure drop through the packed bed reactor, especially at high temperatures and pressures, the pseudo-first-order rate constant was calculated as suggested in reference (15). For gaseous flow through a packed bed reactor, the observed pseudo-first order rate constant is given by the relationship (13)

$$k' = -\ln[1 - X_T]/(W/F_{in})(x_{in}/RT)P_{av}, \quad [17a]$$

where

$$P_{av} = (2/3)(P_{in}^2 + P_{in}P_{out} + P_{out}^2)/(P_{in} + P_{out}). \quad [17b]$$

As mentioned in the previous section, several adjustments are made to the values of the pseudo-first-order rate constants so that they can be compared to rate constants obtained at different regions of the Arrhenius plots and at different catalyst deactivation levels. First, they are corrected to obtain them on the basis of the equivalent weight of fresh catalyst, using Eq. [10] and the information in Table 2 to calculate $k_{obsd}$.

Second, since the concentrations of hydrogen and the total pressures are different during different experimental runs, the pseudo-first-order rate constants are adjusted as shown in Eqs. [15], [16a], and [16b] to calculate $k_{kin}$, $k_{bulk}$, and $k_{knud}$, respectively. The reference values used in these equations are

$$P_{ref} = 40 \text{ psig} \quad [18a]$$

$$C_{H,ref} = 7.675 \times 10^{-5} \text{ g mole/cm}^3. \quad [18b]$$

(The value in Eq. [18b] corresponds to 0.8 mole fraction $H_2$ at $P_{ref}$ and $T_{ref}$ = 200°C.)

A consistent set of adjusted pseudo-first-order rate constants have to be chosen for determining both the low-temperature and the high-temperature asymptotes to the Arrhenius plots. The low-temperature asymptote represents intrinsic kinetic control. Therefore, the low-temperature asymptotes have been drawn through the pseudo-first order rate constants adjusted for kinetic control, $k_{kin}$.

The high-temperature asymptote represents strong pore diffusion influences. However, depending on the mode of diffusion—bulk or Knudsen—the high-temperature asymptote could be drawn through the values adjusted for either bulk diffusion, equation [16a], or Knudsen diffusion, Eq. [16b]. In order to determine the diffusion mechanism in these catalyst samples, we calculated the Knudsen

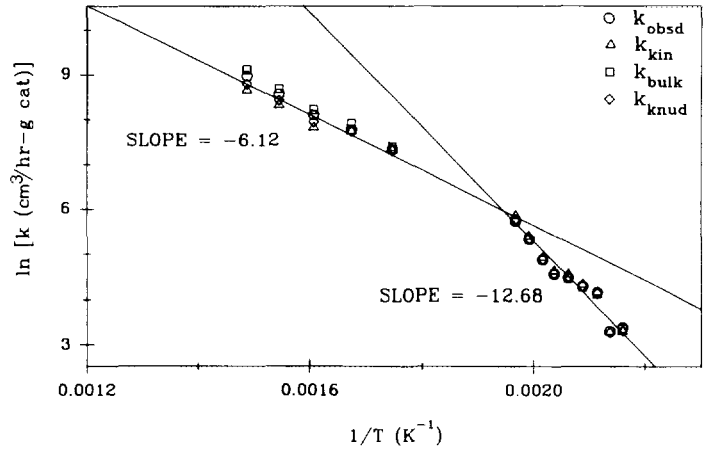


FIG. 2. Arrhenius plot for catalyst sample WIL #4 (142 lb. RSD/lb. cat).

number, $K_1$, at typical reaction conditions in the high-temperature range. $K_1$ is the ratio of the pore diameter to the mean free path of the diffusing molecules,

$$K_1 = d_p/\lambda, \quad [19a]$$

where the mean free path is

$$\lambda = (\pi/4)(c\mu/P) \quad [19b]$$

$$c = (8RT/\pi M_g). \quad [19c]$$

If $K_1$ is greater than 1, bulk diffusion predominates; if less, then Knudsen diffusion is the dominant mechanism. At 350°C (a typical temperature for the high-temperature asymptote), a total pressure of 4 atm, and with the pore diameter taken as that of the fresh catalyst pellet, the calculated value of $K_1$ is 0.6. Hence, diffusion is predominantly by the Knudsen mode. Therefore, the high-temperature asymptote has been drawn through the adjusted rate constants for Knudsen diffusion, $k_{knud}$ of Eq. [16b].

## RESULTS

Experiments with the reactor filled with glass beads, and having a void volume approximately the same as that of the reactor filled with catalyst pellets, showed very little conversion of thiophene, less than 5%, even at the highest temperatures (400–500°C). This indicates that the homogeneous or noncatalytic HDS of thiophene is not significant at the temperatures of this study. The assumption of pseudo-first-order kinetics for thiophene HDS was tested by obtaining thiophene conversions at four or five different flow rates at several temperatures. Thiophene conversions ranged from 10 to 75%, at temperatures in the range 225–425°C. The results indicate that the first-order assumption is indeed valid (13).

Typical Arrhenius plots are shown in Figs. 2–4. All

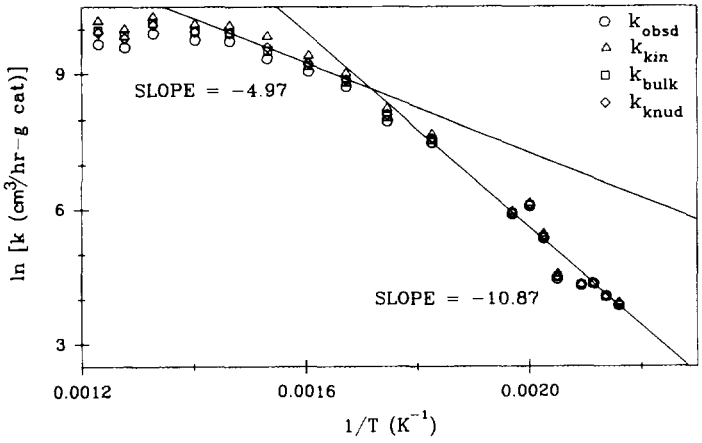


FIG. 3. Arrhenius plot for catalyst sample WIL #1 (1 lb. RSD/lb. cat).

three adjusted values of the pseudo-first-order rate constant are shown, as given by Eqs. [15] and [16]. Recall that these adjustments are in order to compare the observed rate constants obtained at different reaction conditions. Actually, the various adjusted values of the rate constants, at the same temperature, do not differ appreciably from each other. In addition, no matter which adjusted values are used, the Arrhenius plots clearly exhibit distinct regions of different slopes (different apparent activation energies). In other words, the changes in the apparent activation energy of these plots are not artifacts of the adjustments to the observed rate constants. The low- and high-temperature asymptotes are also shown for each Arrhenius plot, using Eqs. [15] and [16b], respectively.

Figure 2 represents the Arrhenius plots for sample WIL #4; plots for WIL #5 and WIL #6 are similar. The slope of the low-temperature asymptote gives an activation energy of approximately 22 kcal/mole. This corresponds to the activation energy of the intrinsic reaction. Similar values of the activation energy have been noted for thiophene HDS in other studies (17). The slopeof the high-temperature asymptote is approximately half that of the low-temperature asymptote, consistent with strong pore diffusion limitations at the high temperatures.

The other Arrhenius plots exhibit some of the same features. The slopes of the low-temperature asymptotes for these Arrhenius plots give approximately the same activation energies as before. Asymptotes at (moderately) high temperatures have slopes half that of the low-temperature asymptotes, again as before. This indicates that reactions at (moderately) high temperatures are in the diffusion-limited region. However, the plots for WIL #1 (Fig. 3) exhibits an additional region with a yet-lower activation energy; the plot for WIL #2 is similar. Finally, the two most-deactivated catalysts, WIL #9 and WIL #12 (Fig. 4), also exhibit a third region, but one with a higher activation energy. We have explained the presence of these additional regions (16, 18). A brief summary of the explanation follows.

The HDS of thiophene was shown to be a two-step series reaction with the two steps having different activation energies. For the slightly deactivated catalysts (e.g., Fig. 3), the highest-temperature region of the Arrhenius plots corresponds to a change in the rate-determining step of the series reaction sequence. On the other hand, strongly deactivated catalysts (e.g., Fig. 4) have appreciable amounts of metal deposits in the outer layers of the catalyst pellet. The major metal compound deposited, iron sulfide, has been shown (by us (18) and others) to possess significant catalytic activity for thiophene HDS. At high temperatures in the region influenced by strong pore diffusion, thiophene HDS takes place mainly in the outer layers of the catalyst pellet, where the iron sulfide is concentrated. This effect gives the third region on the Arrhenius plots for the highly deactivated catalysts.

Experiments with crushed catalyst samples verify that the low-temperature region of the Arrhenius plots is indeed one in which the intrinsic kinetics controls the overall rate of reaction. Figure 5 shows the Arrhenius plot for crushed sample WIL #12 (particle size less than 37 $\mu$m). For comparison, the Arrhenius plot for sample WIL #12 (pellet) is recast here. The rate constants for the two catalysts are comparable at low temperatures. The activation energy observed at low temperatures for the crushed sample is 22 kcal/mole. This is the same as the activation energy observed at low temperatures for all the predeactivated catalyst samples. Therefore, the low-temperature data for the predeactivated catalyst pellets analyzed are in the kinetics-controlled regime. The small increase in the intrinsic rate constant for the crushed catalyst over the pellets can be attributed to pore plugging in the catalyst pellets. Pore plugging would deny access to the reactants to the active sites of the uncrushed pellets, but the accessi-

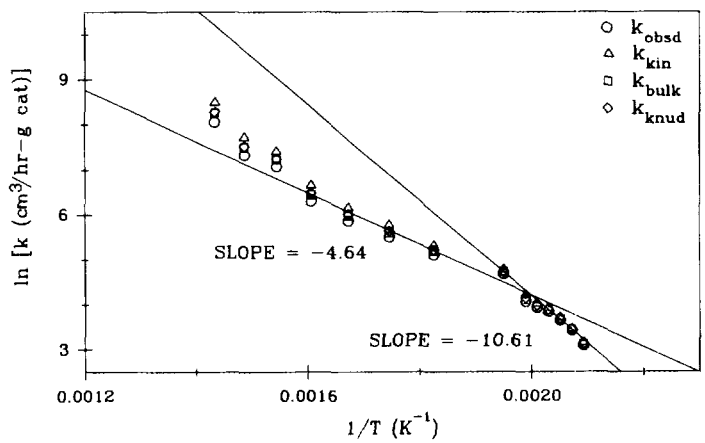


FIG. 4. Arrhenius plot for catalyst sample WIL #12 (506 lb. RSD/lb. cat).

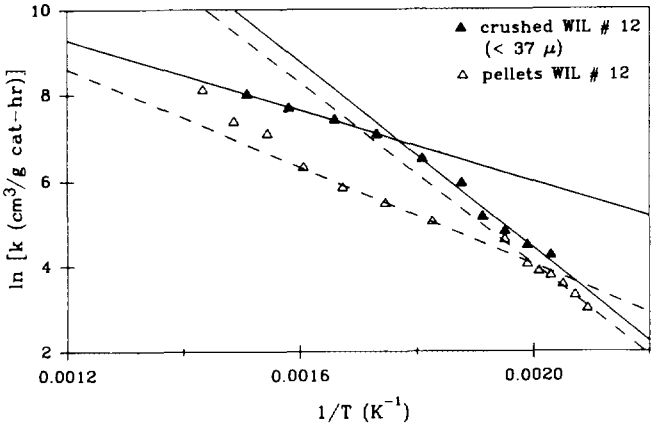


FIG. 5. Arrhenius plot for crushed sample WIL #12 compared to the Arrhenius plot for whole pellets of sample WIL #12.

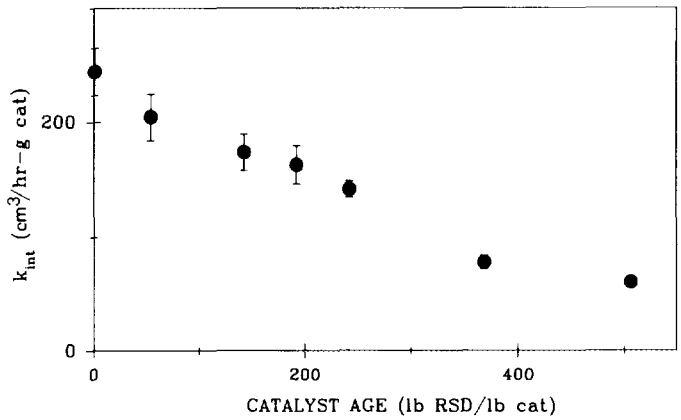


FIG. 7. Intrinsic rate constants $k_{int}$ at 225°C versus catalyst age.

bility of the active sites would be relatively unaffected for the crushed catalyst.

## DISCUSSION

### *Activation Energies for Reaction and Diffusion*

For the reduced quantities $R_k$ and $R_D$ (as defined in Eqs. [11] and [12] to represent the extents of active site suppression and pore choking respectively, the mechanism of reaction over the catalyst should not change as the catalyst deactivates. A change in reaction mechanism is usually indicated by a change in activation energy of the reaction. Figure 6 shows the activation energy for reaction, $E_k$, as determined from the low-temperature asymptotes as a function of catalyst age. Since $E_k$ is approximately the same at all catalyst ages, the reaction mechanism for thiophene HDS does not change with deactivation.

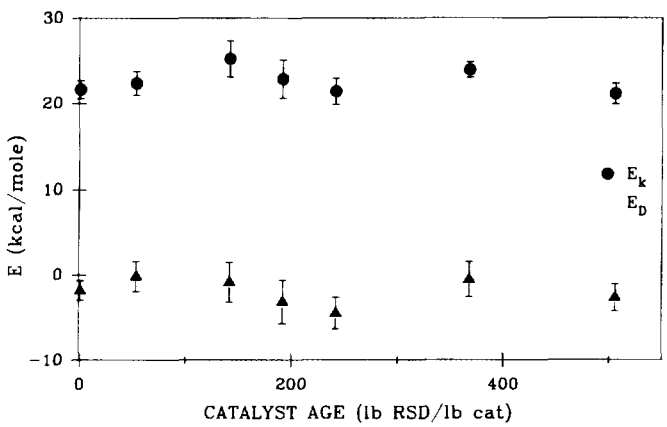


FIG. 6. Activation energies for reaction, $E_k$, and diffusion, $E_D$, versus catalyst age.

The activation energy for diffusion, $E_D$, is also shown in Fig. 6. $E_D$ is calculated from the slopes of the low-temperature and high-temperature asymptotes, $m_L$ and $m_H$, respectively, using Eqs. [3] and [7]. The calculated $E_D$ for the catalyst samples analyzed is nearly zero at all catalyst ages. Considering that $E_D$ is calculated from the least-squares slopes of two asymptotes, the calculated value is close to the normal range of values, 1–4 kcal/mol, as mentioned earlier.

### *Intrinsic Rate Constants*

The low-temperature asymptote of the Arrhenius plots gives $k_{int}$ for all the predeactivated catalyst samples at any temperature directly, from Eq. [9a]. The value of $k_{int}$ can be calculated by extrapolation of the low-temperature asymptote to the desired temperature.

Figure 7 shows the calculated values of $k_{int}$ as a function of catalyst age at 225°C. There is little change in $k_{int}$ upto a catalyst age of 200 lb. RSD/lb. cat. After this catalyst age, however, the value of $k_{int}$ decreases nonnegligibly, reaching approximately 25% of its initial value at 506 lb. RSD/lb. cat. Therefore, up to 200 lb. RSD/lb. cat, suppression of the active sites may be considered to be slight. Beyond this catalyst age, though, site suppression is present.

### *Effective Diffusivities*

The value of $D_{eff}$ for the predeactivated catalyst samples is calculated from both the low- and the high-temperature asymptotes. For samples WIL #4, #5, and #6, Eq. [9b] is used. $D_{eff}$ for other catalyst samples have been evaluated in Refs. (16, 18). Figure 8 shows the calculated values of $D_{eff}$ versus catalyst age at 225°C. The values of $D_{eff}$ decrease continuously with catalyst age. The value of $D_{eff}$ at a catalyst age of 200 lb. RDS/lb. cat is approximately one order of magnitude lower than the value at the start

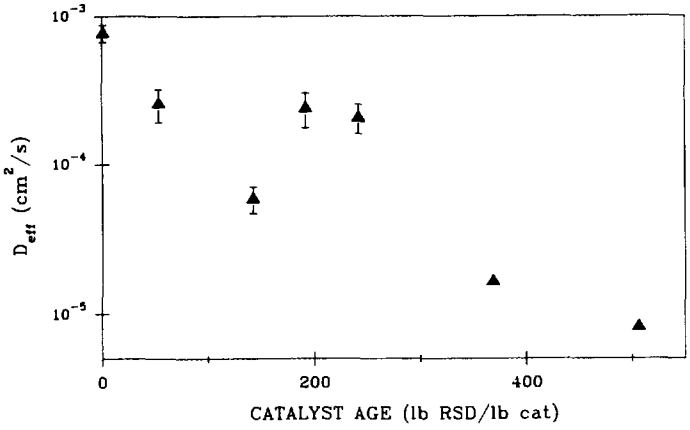


FIG. 8. Effective diffusivities $D_{eff}$ at 225°C versus catalyst age.

of HT, and a second order of magnitude is lost between 220 and 506 lb. RSD/lb. cat. Therefore, pore choking contributes significantly to catalyst deactivation at all catalyst ages.

### *Ratios of Intrinsic Rate Constants and Effective Diffusivities*

The ratios $R_k$ and $R_D$ are dimensionless, and therefore can be compared to each other to determine the relative importance of pore choking and site suppression during catalyst deactivation. Figure 9 shows the ratios at 225°C, plotted on the same scale for comparison.

The two periods of deactivation are more apparent from this figure than from Figs. 7 and 8. Pore choking is the dominant deactivation mechanism upto a catalyst age of 200 lb. RSD/lb. cat. While both site suppression and pore choking contribute to catalyst deactivation at higher catalyst ages, the contribution of pore choking is slightly higher than the contribution of site suppression. Over all

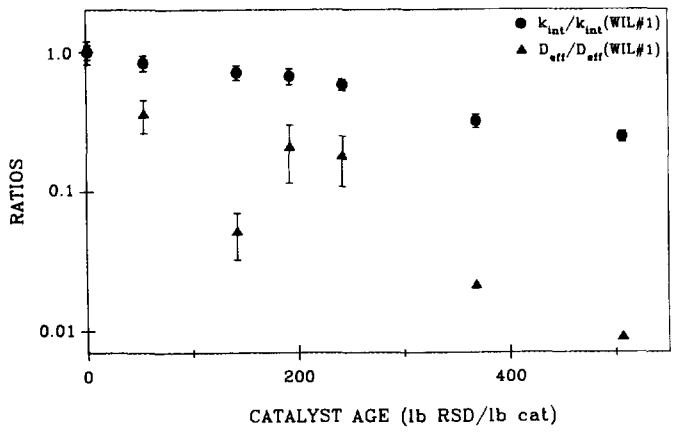


FIG. 9. Ratios of intrinsic rate constants, $R_k$, and effective diffusivities, $R_D$, as compared to sample WIL #1, all at 225°C.

the catalyst samples in this study, the change in $R_D$ is more than an order of magnitude higher than the change in $R_k$. Hence, considering the overall picture, the contribution of pore choking to catalyst deactivation is much more than the contribution of site suppression.

The trends in $k_{int}$ and $D_{eff}$, and hence in the ratios $R_k$ and $R_D$, are similar at thiophene HDS temperatures other than 225°C (13). This is as expected, since we are working with predeactivated catalysts, and the trends in these values should be independent of the temperature at which they are compared.

### *Comparison with Earlier Work*

Stiegel *et al.* (3) have measured pore volumes and average pore diameters of catalyst samples also from Run #242. The pore volumes of the catalysts, as measured by mercury porosimetry, decrease by 33% between the ages of 1–506 lb. RSD/lb. cat. Further, the average pore diameter decreases by 33% between these catalyst ages. These results provide additional evidence of the decline in diffusivity with catalyst age. However, the decreases in pore volumes and diameters indicate a decrease in diffusivity by only 50%, whereas the effective diffusivity is shown in the present work to decrease to 1% of its original value. The much larger changes in the effective diffusivity observed in our study may be due to blockage of closed-end pores, which effect is transparent to mercury porosimetry. Mathematically this effect can be described by an increase of the tortuosity of the catalyst pellet.

Also using the same catalyst samples, Guin *et al.* (5) observe approximately an order of magnitude decrease in $D_{eff}$ between catalyst ages of 1–467 lb. RSD/lb. cat. Guin *et al.* have carried out diffusion experiments, and these can be expected to yield lower values of $D_{eff}$ than those obtained indirectly by Stiegel *et al.* above. However, the use of small inert compounds by Guin *et al.* leads to the measurement of the diffusivity for the entire pellet surface, not the active surface of the catalyst pellet. If the active surface in the pre-deactivated catalyst pellet is nonuniformly distributed, i.e., if deactivation of active sites occurs nonuniformly in the pellet, then the values of $D_{eff}$ obtained by using inert compounds and reactive compounds could be expected to differ. The distribution of the metals deposited in the catalyst pellet during coal-liquid HT has been found to be highly nonuniform (2). This indicates that the larger decrease in $D_{eff}$ can be explained thus.

The diffusivities measured by Guin *et al.* have been in the liquid phase. The mechanism of diffusion in the liquid phase is purely of the bulk mode, which is independent of the diameter of the pores inside the catalyst pellet. However, we have shown earlier that the mechanism of diffusion in the gas-phase reaction of thiophene HDS is

primarily of the Knudsen mode, which is directly proportional to the pore diameter. This could also explain the differences in variation of $D_{eff}$ with catalyst age observed by the two studies.

Stephens and Stohl (6) observed little or no change in the $D_{eff}$ for similar catalysts. An important assumption there is that crushing the catalyst pellet to 75 $\mu$m in diameter eliminates diffusion constraints, allowing the value of $k_{int}$ to be directly measured. However, this may not be the case for highly deactivated catalyst samples; see for example, Fig. 5, where crushing the catalyst pellets to less than 37 $\mu$m does not remove diffusion constraints at temperatures above 300°C. For the case when pore choking is significant, the value of $D_{eff}$ obtained by their method would be apparently greater than the true value, with the relative increase being larger at higher deactivation levels. This could lead to little apparent decrease in diffusivity with deactivation.

Another point not considered by Stephens and Stohl is the catalytic hydrogenation activity of the metal deposits on the catalyst pellet for hydrogenation. Actually iron sulfide, a common deposit on these catalysts, possesses appreciable catalytic activity (18). The highly uneven distribution of this metal compound in the catalyst pellet leads to a nonuniform distribution of activity inside the pellet. The relationship between the effectiveness factor and the Thiele modulus for a uniform pellet, assumed by Stephens and Stohl for calculation of effective diffusivities, does not hold for such a nonuniform pellet. These considerations can explain the differences observed in the trends of $D_{eff}$ with catalyst age.

Stephens and Stohl (6) also observe that the value of $k_{int}$ decreases continuously with catalyst age. These values are for the hydrogenation of pyrene, however, and need not show the same trend as the values for the HDS of thiophene, if the two reactions take place on different sites. The existence of two different sites for HDS and hydrogenation on NiMo catalysts has been suggested by a number of studies (10, 11, 17, 18).

## CONCLUSIONS

The relative importance of the two mechanisms of catalyst deactivation—active site suppression and pore choking—has been determined for the HT of coal-derived liquids. Values of kinetic and mass transfer parameters $k_{int}$ and $D_{eff}$ have been evaluated at various catalyst ages to distinguish between these two mechanisms. The HDS of thiophene, a sulfur-containing compound found in coal-liquids, was carried out over predeactivated catalyst samples obtained from a coal-liquid HT reactor. The age of the catalyst is quantified as the pounds of residuum processed through the hydrotreater per pound of catalyst in the reactor. Pseudo-first-order reaction rate constants for thiophene HDS in excess hydrogen were obtained over a wide temperature range, encompassing both the intrinsic kinetic-control regime and the regime of strong pore diffusion influence. The data were corrected to allow for changes in total pressure, hydrogen concentration and diffusion type over the wide range of conditions used. The values of $k_{int}$ and $D_{eff}$ were determined from the Arrhenius plots.

It should be emphasized that, although the values of the kinetic and mass transfer parameters refer to thiophene, the deactivation of the catalysts has taken place in a commercial-scale treatment facility. Hence the conclusions obtained here involve more than simply studies on model compounds and are applicable to a "real" system.

Two periods of deactivation are observed. Upto a catalyst age of 200 lb. RSD/lb. cat, there is little change in the value of $k_{int}$ but a large decrease in the value of $D_{eff}$. Beyond the age of 200 lb. RSD/lb. cat, there is both a decrease in $k_{int}$ and a decrease in $D_{eff}$. The decrease in $D_{eff}$ is somewhat larger, though, than the decrease in $k_{int}$. Hence, upto a catalyst age of 200 lb. RSD/lb. cat, pore choking is the dominant mechanism of deactivation. At higher catalyst ages, both pore choking and site suppression are responsible for catalyst deactivation, with the effect of pore choking being greater than the effect of site suppression.

## APPENDIX: NOMENCLATURE

| | |
|---|---|
| $A_L$ | Value of low-temperature asymptote ($cm^3$/hr-g cat) |
| $A_H$ | Value of high-temperature asymptote ($cm^3$/h-g cat) |
| $c$ | Average molecular speed (cm/sec) |
| $C_H$ | Hydrogen concentration (mole/$cm^3$) |
| $C_{H,ref}$ | Reference hydrogen concentration (mole/$cm^3$) |
| $d_p$ | diameter of pore (cm) |
| $D_{eff}$ | Effective diffusivity ($cm^2$/sec) |
| $E_D$ | Activation energy of diffusion (kcal/mole) |
| $E_k$ | Activation energy of reaction (kcal/mole) |
| $F_{in}$ | Molar flowrate of thiophene at reactor inlet (mole/hr) |
| $k'$ | Observed pseudo-first-order rate constant ($cm^3$/hr-g cat) |
| $k_{bulk}$ | Adjusted rate constant for bulk diffusion ($cm^3$/hr-g cat) |
| $k_{int}$ | Intrinsic reaction rate constant ($cm^3$/hr-g cat) |
| $k_{kin}$ | Adjusted rate constant for intrinsic kinetics control ($cm^3$/hr-g cat) |
| $k_{knud}$ | Adjusted rate constant for Knudsen diffusion ($cm^3$/hr-g cat) |
| $k_{LH}$ | Langmuir–Hinshelwood reaction rate constant (mole/hr-g cat-$atm^2$) |

| | |
|---|---|
| $k_{obsd}$ | Adjusted reaction rate constant defined in Eq. [10] ($cm^3$/hr-g cat) |
| $k_s$ | Adsorption constant for hydrogen sulfide ($atm^{-1}$) |
| $k_T$ | Adsorption constant for thiophene ($atm^{-1}$) |
| $K_I$ | Knudsen number |
| $L$ | Length parameter of pellet |
| $m_L$ | Slope of low-temperature asymptote |
| $m_H$ | Slope of high-temperature asymptote |
| $M_g$ | Molecular weight (g/g mole) |
| $P_{av}$ | Average pressure in reactor (atm) |
| $P_H$ | Partial pressure of hydrogen (atm) |
| $P_{in}$ | Pressure at reactor inlet (atm) |
| $P_{out}$ | Pressure at reactor outlet (atm) |
| $P_s$ | Partial pressure of hydrogen sulfide (atm) |
| $P_t$ | Total Pressure in reactor (atm) |
| $P_{t,ref}$ | Reference total pressure in reactor (mole/$cm^3$) |
| $P_T$ | Partial pressure of thiophene (atm) |
| $r_T$ | Rate of reaction of thiophene (mole/hr-g cat) |
| $R$ | Gas constant (kcal/mole/K) |
| $R_k$ | Ratio of intrinsic reaction rate constants |
| $R_D$ | Ratio of effective diffusivities |
| $T$ | Temperature (K) |
| $W$ | Weight of catalyst (g) |
| $x_{in}$ | Mole fraction of thiophene at reactor inlet |
| $X_T$ | Thiophene conversion |
| $\eta$ | Effectiveness factor of catalyst pellet |
| $\phi$ | Thiele modulus of catalyst pellet |
| $\rho_p$ | Density of catalyst particle (g/$cm^3$) |
| $\pi$ | Deactivation level of catalyst (lb. RSD/lb. cat) |
| $\pi_{ref}$ | Reference deactivation level of catalyst (lb. RSD/lb. cat) |
| $\lambda$ | mean free path (cm) |
| $\mu$ | Viscosity (Poise) |

## ACKNOWLEDGMENTS

This work was supported by USDOE/PETC under No-Cost Cooperative Agreement Grant DE-AC22-88PC-79808 and by the West Virginia University Energy and Water Research Center under Project CTL-12-88. Dr. Richard Tischer of PETC provided the samples of predeactivated catalyst, Dr. N and Narain was of invaluable help in the early stages of this work, and Dr. Gary Stiegel provided help throughout the work.

## REFERENCES

1. Schindler, H. D., "Coal Liquefaction—A Research Needs Assessment," Vol. 2, DOE/ER-0400, U.S. Department of Energy, Washington, DC, 1989.
2. Stohl, F. V., Stephens, H. P., *Ind. Eng. Chem. Res.* **26,** 2466 (1987).
3. Stiegel, G. J., Tischer, R. E., Cillo, D. L., and Narain, N. K., *Ind. Eng. Chem. Prod. Res. Dev.* **24,** 206 (1985).
4. Aris, R., "The Mathematical Theory of Diffusion and Reaction in Permeable Catalysts," Vol. 1. Oxford, New York, 1975.
5. Guin, J. A., Tsai, K. J., and Curtis, C. W., *Ind. Eng. Chem. Process. Des. Dev.* **25,** 515 (1986).
6. Stephens, H. P., and Stohl, F. V., *Prepr.—Am. Chem. Soc. Div. Fuel Chem.* **29,** 79 (1984).
7. Dadyburjor, D. B., *J. Catal.* **79,** 222 (1984).
8. Bellare, A., and Dadyburjor, D. B., *J. Catal.* **140,** 510 (1993).
9. Satterfield, C. N., "Mass Transfer in Heterogeneous Catalysis." MIT Press, Cambridge, MA, 1970.
10. Satterfield, C. N., and Roberts, G. W., *AIChE. J.* **14,** 159 (1968).
11. Ihm, S-K. Moon, S-J., and Choi, H-J., *Ind. Eng. Chem. Res.* **29,** 1147 (1990).
12. Roberts, G. W., and Satterfield, C. N., *Ind. Eng. Chem. Fundam.* **5,** 317 (1966).
13. Raje, A. P., Ph.D. Dissertation, West Virginia University, 1992.
14. Technical Progress Report, "Run 242 with Illinois #6 Coal," DOE/PC/50041-19, U.S. Department of Energy, Washington, DC, July 1983.
15. Fogler, H. S., "Elements of Chemical Reaction Engineering." Prentice–Hall, Englewood Cliffs, NJ, 1986.
16. Raje, A., and Dadyburjor, D. B., *Chem. Eng. Commun.*, in press.
17. Owens, P. J., and Amberg, C. H., *Adv. Chem. Ser.* **33,** 182 (1961).
18. Raje, A., and Dadyburjor, D. B., *Ind. Eng. Chem. Res.*, **32,** 1637 (1993).